Talanta 131 (2015) 243–248

Contents lists available at ScienceDirect

Talanta

journal homepage: www.elsevier.com/locate/talanta

Hydrogen peroxide biosensor based on microperoxidase-11 immobilized on flexible MWCNTs-BC nanocomposite film

Bingyan Zhang [a], Jianhai Zhou [b], Shaohui Li [a], Xiaofan Zhang [a], Dekang Huang [a], Yahui He [a], Mingkui Wang [a], Guang Yang [b,*], Yan Shen [a,*]

[a] Wuhan National Laboratory for Optoelectrosnics, School of Optoelectronic Science and Engineering, Huazhong University of Science and Technology, Wuhan 430074, P.R. China

[b] National Engineering Research Center for Nano-Medicine, College of Life Science and Technology, Huazhong University of Science and Technology, Wuhan, 430074, P.R. China

ARTICLE INFO

Article history:
Received 20 March 2014
Received in revised form
8 July 2014
Accepted 10 July 2014
Available online 18 July 2014

Keywords:
Biosensor
Bacterial cellulose
Multi-walled carbon nanotubes
Microperoxidase-11
H_2O_2 detection

ABSTRACT

In the present work, we report on an experimental study of flexible nanocomposite film for electrochemical detection of hydrogen peroxide (H_2O_2) based on bacterial cellulose (BC) and multi-walled carbon nanotubes (MWCNTs) in combination with microperoxidase-11 (MP-11). MWCNTs are used to functionalize BC and provide a flexible conductive film. On the other hand, BC can improve MWCNTs' biocompatibility. The investigation shows that MP-11 immobilized on the flexible film of MWCNTs–BC can easily present a pair of well-defined and quasi-reversible redox peaks, revealing a direct electrochemistry of MP-11 on the nanocomposite film. The apparent heterogeneous electron-transfer rate constant k_s is estimated to be 11.5 s^{-1}. The resulting flexible electrode presents appreciated catalytic properties for electrochemical detection of H_2O_2, comparing to traditional electrodes (such as gold, glassy carbon electrode) modified with MP-11. The proposed biosensor exhibits a low detection limit of 0.1 μM (at a signal-to-noise ratio of 3) with a linear range of 0.1–257.6 μM, and acquires a satisfactory stability.

© 2014 Elsevier B.V. All rights reserved.

1. Introduction

The detection of hydrogen peroxide (H_2O_2) is of great importance in food and environmental analyses, diagnosis, industry, pharmaceutical laboratories and biological studies. H_2O_2 is harmful for biological systems and appears to be involved in the neuropathology of central nervous system diseases. It has been reported that H_2O_2 induces oxidative stress in CGNs, involving both apoptotic and necrotic death [1]. The increased production of H_2O_2 has been implicated in the pathogenesis of several neurodegenerative diseases, including Parkinson's and Alzheimer's diseases, as well as in the damage produced by ischemia and reperfusion [2]. In the past years, various methods have been developed for determination of H_2O_2, including oxidimetry [3], chemi-luminescence [4,5], surface plasmon resonance [6,7], fluorescence [8], and so on. Among these methods, the electrochemical method offers advantages including simplicity, high reliability, sensitivity, low cost and ease of use [9,10].

In recent years, great attention has been attracted to carbon nanotubes (CNTs) for biosensors application because of its unique physical, electronic and chemical properties [9–11]. Several studies have demonstrated that CNTs have excellent electro-catalytic abilities and antifouling properties and have the ability to promote electron transfer reactions when they were used as electrode material in electrochemical reactions [12–15]. CNTs have been widely used to detect several biomolecules such as dopamine, H_2O_2 and glucose [16–19]. However, most of CNTs without modification have limitation of poor dispensability and biocompatibility. In order to solve these problems, surface modification with surfactant and chitosan and other methods were introduced [20,21]. Recently, bacterial cellulose (BC) has been received much attention due to its biocompatibility, ultrafine network, and biodegradability compared with plant cellulose [22,23]. BC can be produced with different microorganisms [24]. Biosensors based on nanostructured carbon materials and BC might benefit from their complementary advantage to enhance their biocompatibility. Yoon and Zhou reported that the insulating BC could become conductive by incorporation of CNTs (1.4×10^{-1} S cm^{-1}) and graphite nanoplatelets (1.2 S cm^{-1}), respectively [25,26]. It was demonstrated that horseradish per-oxidase (HRP) immobilized on gold nanoparticles–bacteria cellulose nanofibers nanocomposite showed high performance of detecting H_2O_2 with a wide range of concentration from 0.3 μM to 1.00 mM, and a low detection limit of 0.1 μM based on $S/N=3$ [27]. Recently, flexible biosensors that can

* Corresponding authors.
E-mail addresses: yang_sunny@yahoo.com (G. Yang), ciac_sheny@mail.hust.edu.cn (Y. Shen).

http://dx.doi.org/10.1016/j.talanta.2014.07.027
0039-9140/© 2014 Elsevier B.V. All rights reserved.

accommodate dramatic shape changes have got a fast development for the minimally invasive implantable devices and compact diagnostic platforms. Kim et al. first reported a flexible and ultrathin BC–CNTs film as a candidate to the ubiquitously employed glucose oxidase electrodes for glucose detection [28], which demonstrated a successful application for BC as a flexible matrix electrode in bioelectrochemistry.

Several proteins can be used to construct H_2O_2 biosensors, such as microperoxidase-11 (MP-11), HRP, myoglobin and hemoglobin [29,30]. MP-11 is a widely used enzyme for the construction of H_2O_2 biosensors due to its high purity, sensitivity and low cost [31,32], Herein, we communicate preliminary results on the application of MWCNTs to functionalize BC and provide a flexible conductive film. The resulting flexible MWCNTs–BC film can effectively immobilize the MP-11 and improve the stability of the biosensor compared to the bare MWCNTs, showing high performance for electrochemical detection of H_2O_2.

2. Experimental

2.1. Reagents and apparatus

MWCNTs (diameter 10–20 nm, length 2 μm, purity 97%) were purchased from Chengdu Organic Chemicals Co. Ltd. A fresh aqueous solution of H_2O_2 was prepared daily. All the reagents were of analytical grade and used without purification. The supporting electrolyte used for the electrochemical studies was 0.1 M phosphate buffered solutions (pH 7.0) which were prepared from stock solutions of 0.1 M NaH_2PO_4, 0.1 M Na_2HPO_4, 0.1 M NaCl. H_2O (18 Ω M) was obtained from a Millipore-Q water purification system.

The morphology of prepared materials was examined on a field emission scanning electron microscopy (FE-SEM) (Hitachi S-4800 electron microscope, Hitachi, Japan). The infrared spectra were carried out using a VERTEX 70 Fourier Transform Infrared spectrometer. Raman spectra was carried out using LabRAM HR800 Confocal Raman Spectroscopy, and UV–vis absorption spectroscopic measurements were carried out using a Hitachi U-3300 spectrophotometer.

The measurements of cyclic voltammetry (CV) and amperometric *I–t* curve (*I–t*) were carried out using a CHI 920C electrochemical analyzer (CHI). A conventional three electrode cell consisting of an Ag/AgCl (3 M KCl) reference electrode and a twisted platinum wire as an auxiliary electrode was employed. All experiments were performed at room temperature.

2.2. Preparation of MWCNTs–BC and MP-11/MWCNTs–BC film flexible electrode

Gluconacetobacter xylinum (ATCC53582) was used for the biosynthesis of BC [33]. The bacterium was cultured in a Hestrin and Schramm (HS) medium, which was composed of 2% (wt) glucose, 0.5% (wt) yeast extract, 0.5% (wt) peptone, 0.27% (wt) disodium phosphate, and 0.15% (wt) citric acid. After having been incubated statically at 26 °C for 14 days, the BC membranes were formed and then dipped in distilled water and NaOH solution, respectively. The pH was lowered to 7.0 by washing with distilled water. The purified cellulose pellicles were stored in distilled water at 4 °C to avoid drying. Then some pieces of the purified cellulose pellicles were put into the sulfuric acid solution (40%). Afterwards, the obtained BC whiskers were centrifuged and dialyzed in deionized water successively for further purified to get 0.3% BC whiskers aqueous solution. 5 mg mL^{-1} MWCNTs aqueous suspension was added into BC whiskers aqueous solution to get a uniformly mixed solution and then put it filtered. Finally, the flexible conductive MWCNTs–BC films were produced, and the mass ratio of BC and MWCNTs was 1:10. Then the film was cut into suitable shape. The obtained flexible film was immersed in the PBS solution containing 1 mg mL^{-1} MP-11 (pH 7.0) for 16 h, and then the MP-11 molecular was immobilized onto the surface of MWCNTs–BC film. The final modified flexible film was washed with deniozed water for several times.

2.3. Platelet adhesion studies

The platelet-rich plasma (PRP) was purchased from Pingrui Biotechnology Company (Beijing, China), and the experimental method has been reported by Meyerhof [23c]. Briefly, BC–MWCNTs was preincubated at 37 °C for 20 min. BC–MWCNTs film previously conditioned in phosphate-buffered saline (PBS, containing 10 mM phosphate, 138 mM sodium chloride, and 2.7 mM potassium chloride, pH 7.4) for 3 days were immersed in PRP for 2 h at 37 °C. It was then rinsed in PBS and fixed in a PBS solution containing 2.0% (w/v) glutaraldehyde for 2 h at room temperature. Samples were dehydrated by immersion in serial dilutions of ethanol (30, 50, 70, 90, and 95% v/v), two immersions in absolute ethanol.

3. Results and discussion

3.1. Characterization of the MWCNTs–BC and MP-11/MWCNTs–BC flexible film electrode

The surface morphology of MWCNTs, BC and MWCNTs–BC films were examined by field emission scanning electron microscopy (FE-SEM). The pure MWCNTs with a diameter of about 15–20 nm was evenly spread out, that result in a uniform sample as shown in Fig. 1(a). BC whisker film with ultra-fine network is shown in Fig. 1(b), which leads it to be a good candidate for flexible substrate. Fig. 1c presented the morphology of MWCNTs–BC composite film. It was observed that the diameter of MWCNTs was obviously bigger than BC, and MWCNTs were well-incorporated and distributed within the BC. The BC hydrogel itself works as a nano-sized filter. CNTs efficiently infiltrated into a network of BC when they were filtered though BC hydrogel by vacuum [28].

Fig. 1(d) shows the tensile property for the flexible film substrate tested by HY-0230 electronic universal material testing machine. The result demonstrated that the max stress was about 52.36 MPa for the flexible film with a stretch distance of 1.1 mm, although the thickness of the BC–MWCNTs film was only about 135.2 μm. It indicated that the flexible film performed a good mechanical property.

Fourier transform infrared (FTIR), Raman, and UV−visible spectrum measurements were performed to clearly characterize MWCNTs–BC film. As shown in Fig. 2a, the appearance of the peaks at 1305, 1418, 1625, 1717, 2886 and 3220 cm^{-1} were assigned to C–O, $-CH_2-$, C═C, –COOH, C–H and O–H vibrations, respectively. MP-11 molecular has functional groups, including –COOH, O–H, and $-NH_2$. It is worthy noted that the carboxyl group from MWCNTs induced by concentrated nitric acid (HNO_3, 68%) treatment is beneficial to the adsorption of MP-11onto MWCNTs surface. and the hydroxyl group from BC is beneficial to the combination to MWCNTs. Fig. 2b shows Raman spectra of MWCNTs–BC film, exhibiting two prominent peaks at 1363 and 1596 cm^{-1}, corresponding to the disorder (D band) and the crystalline (G band) graphite, respectively. This indicates the structure of MWCNTs is not affected by BC. The UV–visible spectrum revealed that MP-11/MWCNTs–BC film presents a Soret band at 408 nm. The corresponding Soret band of MP-11 in solution with 0.2 μM was found at 402 nm (Fig. 2c). The bathochromic

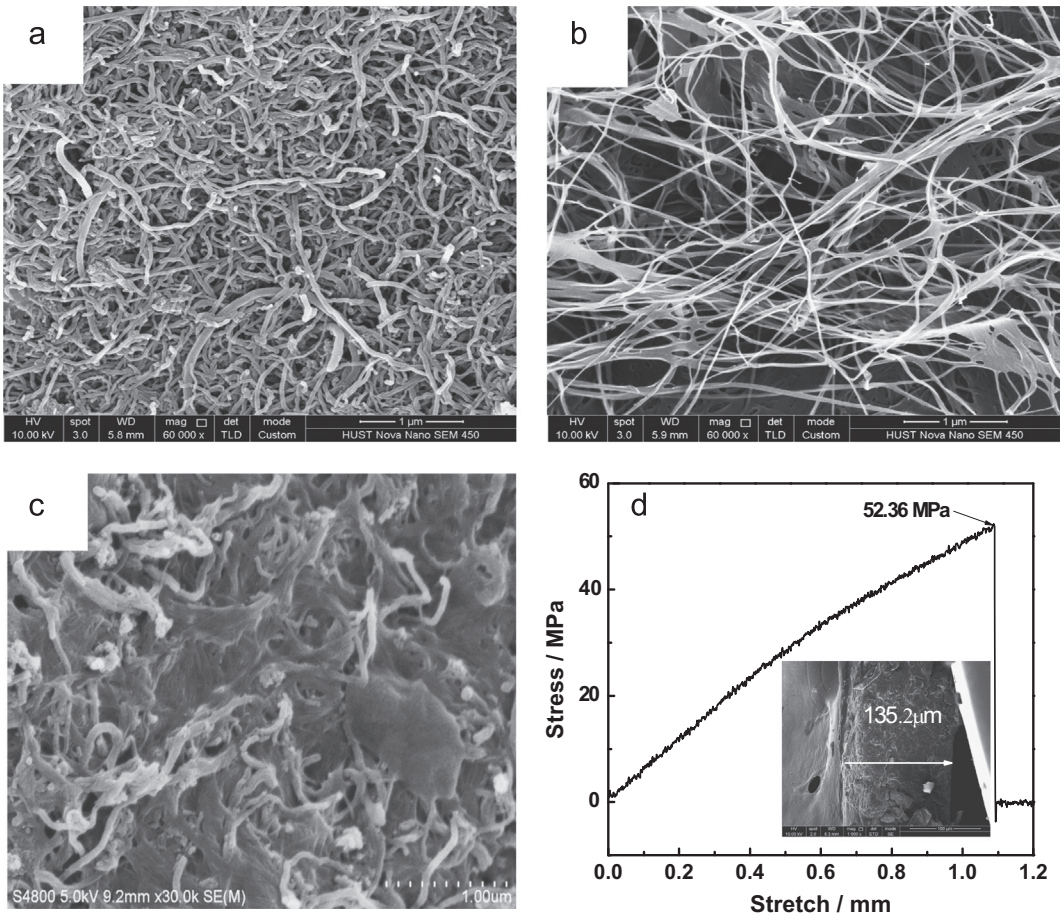

Fig. 1. Field-emission scanning electron micrographs: (a) MWCNTs, (b) pure BC, (c) MWCNTs–BC film, and (d) tensile properties test and the cross section of MWCNTS–BC film.

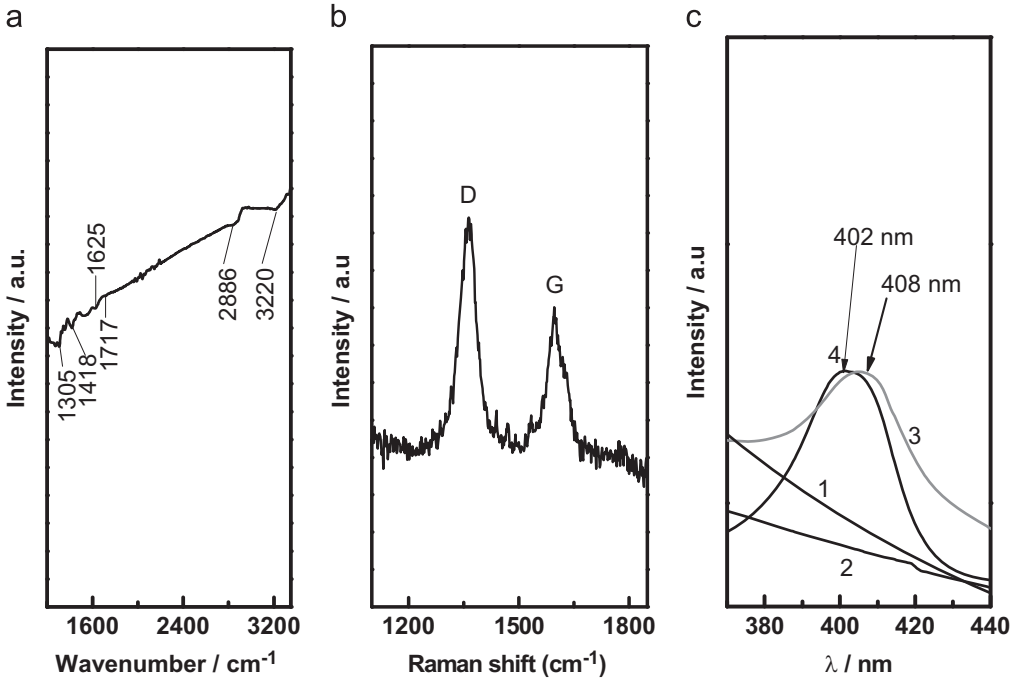

Fig. 2. Normalized intensity of (a) Fourier transform infrared spectra, (b) Raman spectra for BC–MWCNTs, and (c) UV–vis absorption spectra of 1-BC, 2-MWCNTs-BC, 3-MP-11/MWCNTs–BC and 4-MP-11 aqueous solution with 0.2 μM.

shift may be attributed to the aggregation of the adsorbed MP-11 molecules onto substrate [34,35]. The blank experiments on BC and MWCNTs–BC samples presented featureless adsorption in the wavelength range. This result indicated that the flexible composite electrode of MWCNTs–BC was an ideal substrate for adsorption of MP-11 molecules.

3.2. Electrochemical characterization of MP-11 on the flexible MWNTs–BC film electrode

Fig. 3a and b shows the cyclic voltammograms (CVs) obtained at the MWCNTs (dotted line), MP-11/MWCNTs film electrode (dashed line) and MP-11/MWCNTs–BC film electrode (solid line) in 0.1 M N_2-saturated PBS solution (pH 7.0) with and without 2 mM H_2O_2 at a scan rate of 50 mV s^{-1}. CV of MP-11/MWCNTs–BC electrode clearly illustrated a pair of redox peaks at a potential ($E^{0'}$) of −0.33 V with a very low peak to peak separation (ΔE_p) of 50 mV. Under the similar condition, MP-11/MWCNTs presented a wider ΔE_p (Fig. 3a). Obviously, this redox couple corresponds to the direct electron transfer (DET) of MP-11 onto MWCNT–BC film electrode. Meanwhile, MP-11/MWCNTs–BC electrode showed a better catalytic performance to H_2O_2 compared to MP-11/MWCNTs and MWCNTs electrode (Fig. 3b). The effect of scan rate on the voltammetric response of MP-11 was examined in 0.1 M N_2-saturated PBS of pH 7.0. A good liner relationship between the peak currents versus scan rates (Fig. 3c, inset) indicates the electron transfer of the flexible electrode being a surface-controlled process. The amount of electro-active enzyme on the electrode surface (Γ) can be evaluated from the slope of peak currents plotted versus scan rate by the following Eq. (1) [36]:

$$I_p = n^2F^2\upsilon A\Gamma/(4RT) \quad (1)$$

where υ is the scan rate, A is the active area of the working electrode, n is the number of electron per reactant molecule, respectively. F, R and T are the constants. In the present case, the calculated surface coverage for the electro-active species was 1.17×10^{-9} mol cm^{-2}, which is higher than MP-11/MWCNTs (8.4×10^{-10} mol cm^{-2}) [31], MP-11/AuNPs/MWCNTs (5.93×10^{-10} mol cm^{-2}) [32]. This result could be caused by the network structure of BC, which promotes the adsorption of MP-11 onto the MWCNTs with three-dimensional microstructure. As shown in Fig. 3c, both I_{pa} and I_{pc} increased linearly upon increasing the scan rates from 10 to 200 mV s^{-1}. For scan rates from 0.01 to 1.2 V s^{-1}, the electrochemical response of MP-11 shows a quasi-reversible process. With the increasing of the scan rate, the reduction peak shifted negatively and the oxidation peak shifted positively with ΔE less than 200 mV. According to the Laviron's equation for quasi-reversible thin-layer electrochemistry when the $n\times\Delta E <$ 200 mV, the apparent heterogeneous electron transfer rate constant (k_s) could be calculated with the following equations [37]:

$$E_{pc} = E^{0'} - \frac{2.3RT}{\alpha nF}\log\ \upsilon \quad (2)$$

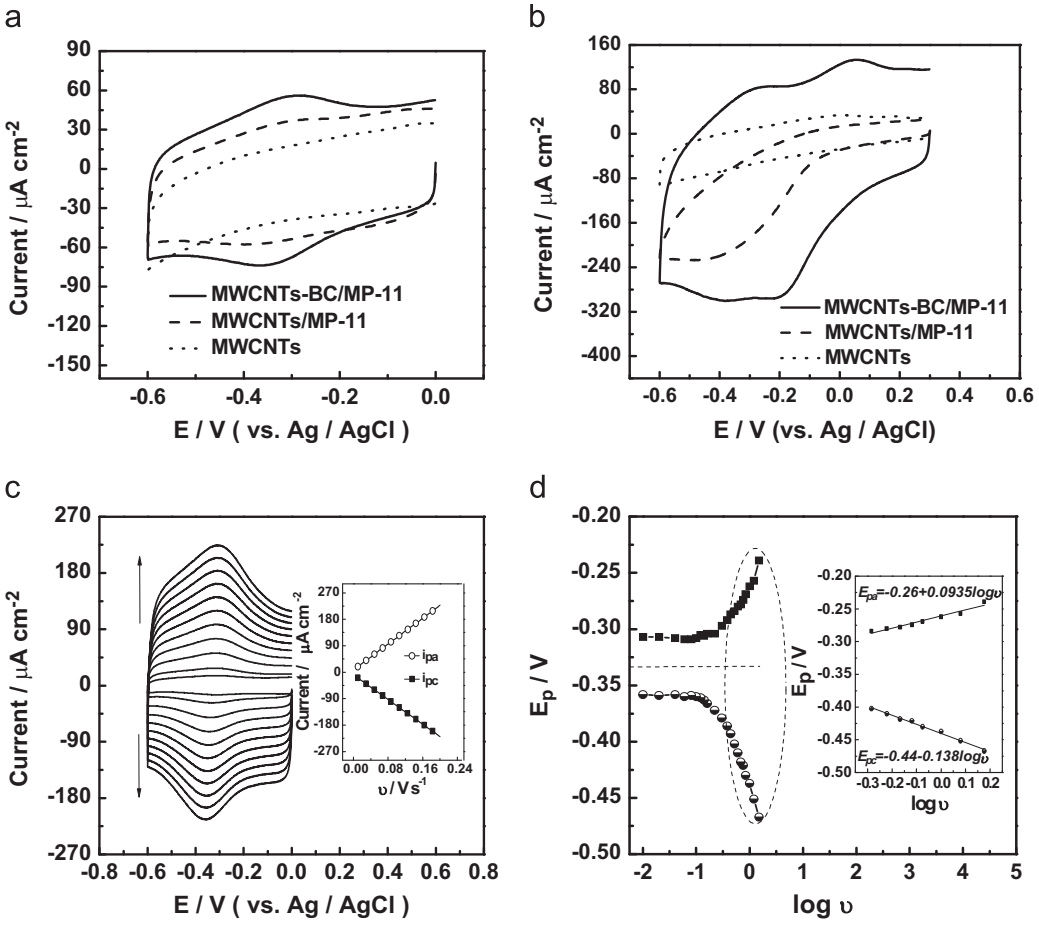

Fig. 3. Cyclic voltammetric responses at MWCNTs–BC film (dot line), MP-11/MWCNTs film electrode (dash line), and MP-11/MWCNTs–BC film electrode (solid line), in N_2-saturated solution (0.1 M PBS, pH 7.0), without H_2O_2 (a), and with 2 mmol L^{-1} H_2O_2 (b), scan rate, 50 mV s^{-1}, (c) CVs of MP-11/MWCNTs-BC film in 0.1 M PBS (pH 7.0) at different scan rates (from inner to outer: 10, 20, 40, 60, 80, 100, 120, 140, 160, 180,200 mV s^{-1}), in N_2-saturated solution (0.1 M PBS, pH 7.0). Inset is the plot of cathodic and anodic peak current vs. scan rate; (d) plots of anodic peak potential and cathodic peak potential against the logarithm of scan rate. Inset is linear dependence of E_{pa} and E_{pc} on log υ.

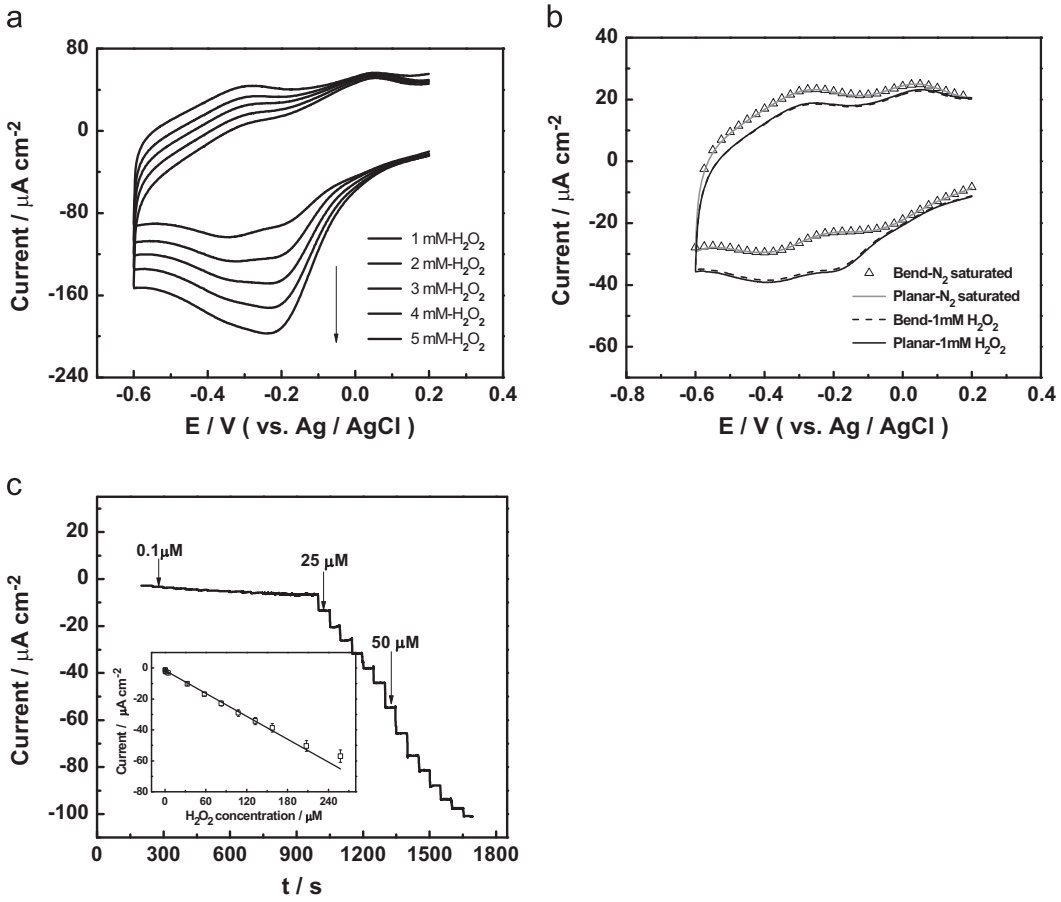

Fig. 4. Cyclic voltammograms of MP-11/MWCNTs–BC film electrode in N_2-saturated PBS solution (0.1 M, pH 7.0), scan rate, 50 mV s^{-1}: (a) with different concentrations of 1 mmol, 2 mmol, 3 mmol, 4 mmol, 5 mmol H_2O_2, and (b) with 1 mM H_2O_2 at two different shapes of bend and planar; (c) amperometric *I–t* response of the hydrogen peroxide biosensor upon addition of H_2O_2, applied potential of −0.3 V. Inset is the linear relationship between catalytic current and the concentration of H_2O_2, in N_2-saturated solution (0.1 M PBS, pH 7.0).

$$E_{pa} = E^{0'} - \frac{2.3RT}{(1-\alpha)nF}\log\ \upsilon \tag{3}$$

$$\log\ k_s = \alpha\log(1-\alpha) + (1-\alpha)\log\ \alpha - \log\frac{RT}{\mathrm{nF}\upsilon} - \frac{nF\Delta E_{pa}(1-\alpha)}{2.3RT} \tag{4}$$

The relationship between ΔE_p and log υ was calculated and shown in Fig. 3d. From the slope and the intercept, the values of n and α were evaluated to be 1.06 and 0.4, respectively, indicating a revisable one electron concerned electrochemical reaction. From the eq. (4), the value of k_s was calculated to be 11.5 s^{-1}. This is close to the best result among the previous reports [31,34]. The large rate constant informs a fast electron transfer between redox active sites of enzyme and the MWCNTs–BC flexible electrode surface. This result could be attributed to MP-11 remains highly redox activity due to the strong hydrophilic property of BC, which enhances the biocompatibility of BC–MWCNTs film. The assessment for the biocompatibility of the composite film has been performed using platelet adhesion study [23b,23c]. Fig. S1 shows the morphology of bare MWCNTs and MWCNTs–BC composite film before and after 2 h contact with platelet-rich plasma (FRP). We can clearly see that the morphology of MWCNTs–BC composite film has no any change after 2 h contact with platelet. However, the morphology of bare MWCNTs has a significant change. It means that more platelet adhered to the bare MWCNTs film, but no platelet adhered to MWCNTs–BC composite film. This confirmed that BC has big effect on the biocompatibility of the composite film.

3.3. Electrochemical detection of H_2O_2 on the flexible MP-11/MWNTs–BC film electrode

Fig. 4a shows the electro-catalytic response of the prepared flexible electrode towards H_2O_2 in 0.1 M N_2-saturated PBS. With a consecutive addition of H_2O_2 from 1 mM to 5 mM, the cathodic peak current increased. It is significant that there is nearly no difference in the cyclic voltammetric response for the flexible electrodes at a bended and planar shape in N_2-saturated solution (0.1 M PBS, pH 7.0) with or without H_2O_2 (Fig. 4b). The first redox couple near 0 V (vs. Ag/AgCl) can be due to MWCNTs, the other one near at −0.3 V (vs. Ag/AgCl) being the quasi-reversible process of MP-11. And the peak at −0.2 V (vs. Ag/AgCl) is from the reduction of H_2O_2. Fig. 4c displays the amperogram at a MP-11/MWCNT–BC film electrode with an applied electrode potential (E_{app}) of −0.3 V. H_2O_2 solution was injected sequentially into the continuously stirred PBS at regular intervals (50 s). Well-defined amperometric responses were observed for the each addition of H_2O_2. The amperometric response current increased linearly with H_2O_2 concentration increasing in the ranges of 0.1–257.6 μM as shown in the calibration plot (Fig. 4c). The linear regression equation can be expressed as I_p (μA cm^{-2}) = −1.53–0.247[H_2O_2] (μM) (R=0.998). The limit of detection (LOD) and sensitivity were calculated to be 0.1 μM and 0.247 A mol^{-1} cm^{-2} based on a signal/noise ratio of 3, suggesting that H_2O_2 could be easily detected at a very low concentration using the flexible film electrode. The fabricated sensor exhibited a wide linear range of 0.1–257.6 μM for H_2O_2 detection compared with that of MP-11/

MWCNTs (3.3–38.4 μM) [31], HRP–PTBA@RTIL (5–175 μM) [38], Hb–AgNPs/CS (0.75–216 μM) [39] and HRP–SnO_2 nanorod array (0.8–35 μM) [40]. In addition, the flexible electrode possessed low detection limit of 0.1 μM, comparatively lower than that of MP-11/MWCNTs (0.7 μM) [31], MP-11-DMPG-G (0.72 μM) [35], HRP–Sb-doped SnO_2 (0.8 μM) [41], HRP–SnO_2 nanorod array (0.2 μM) [40].

The apparent Michaelis–Menton constant (K_M) as one of indication of the enzyme–substrate kinetics, can be estimated with the Lineweaver–Burk equation [42]

$$1/I_{ss} = 1/I_{max} + (K_M/I_{max})(1/C_{H_2O_2}) \quad (5)$$

where I_{ss} is the steady-state current after the addition of substrate, C is the bulk concentration of the substrate, I_{max} is the maximum current measured under saturated substrate condition, respectively. The K_M value for MP-11/MWCNTs–BC film electrode for H_2O_2 detection was calculated to be 0.419 mM. This result is lower than that of MP-11/MGN-CHI/Au (0.54 mM) [43]. The low value of K_M indicates that MP-11 molecules on the BC–MWCNTs thin films retain their bioactivity and have high affinity for H_2O_2.

3.4. Reproducibility and stability studies

The reproducibility of the biosensors was evaluated with five electrodes via comparing their amperometric current response to H_2O_2 independently. The result showed a good reproducibility with a relative standard deviation of 2.67% for the currents determined at a H_2O_2 concentration of 2.0 mM. In order to measure the stability of the system, the flexible MP-11/MWCNTs–BC film electrode was examined by monitoring the remained amount of current response for amperometric I–t response of the H_2O_2. It was found that the peak current for 25 μM H_2O_2 reduction retained 94% of its initial value after bending for 2 days, but only 82% for MP-11/MWCNTs electrode. This indicates that he adsorbed MP-11 on the surface of MWCNTs–BC film electrode is more stable compared with the pure MWCNTs film electrode.

4. Conclusion

In summary, the present study has demonstrated a flexible film electrode based on MP-11 and MWCNTs–BC nanocomposite film for electrochemical detection of H_2O_2. The obtained flexible film electrode, taking advantage of BC's unique three-dimensional structure and biocompatibility, provides a suitable microenvironment for immobilization of MP-11 and retaining its intrinsic structure and biological activity. The MP-11 immobilized on flexible MWCNTs–BC film electrode has realized its direct electrochemistry and shows a good stability and redox activity. The kinetic rate constants ($k_s = 11.5\ s^{-1}$, $\alpha n = 0.4$) and a detection limit as low as 0.1 μM are obtained. This facile, general and inexpensive approach for redox proteins immobilization is applied as a promising platform for the fabrication of biosensors and bioelectronic devices.

Acknowledgments

Financial support from the 973 Program of China (2013CB922104, 2014CB643506, 2011CBA00703), the NSFC (21103057, 21161160445, 21173091), the Fundamental Research Funds for the Central Universities (HUST: CXY12Q022), is gratefully acknowledged. The authors thank the Analytical and Testing Centre at the HUST for performing characterization of various samples. Y. Shen thanks Oldenburg University for supporting visiting. Thanks Professor Jianhua Xiao, who has provided a lot of help for this work.

Appendix A. Supporting information

Supplementary data associated with this article can be found in the online version at http://dx.doi.org/10.1016/j.talanta.2014.07.027.

References

[1] A.A. Fatokun, T.W. Stone, R.A. Smith, Brain Res. 1132 (2007) 193–202.
[2] E.A. Mazzio, K.F. Soliman, Neurochem. Res. 28 (2003) 733–741.
[3] E.C. Hurdis, H. Romeyn, J. Anal. Chem. 26 (1954) 320–325.
[4] G.L. Kok, T.P. Holler, M.B. Lopez, A.H. Nachtrieb, M. Yuan, Environ. Sci. Technol. 12 (1978) 1072–1076.
[5] Y.B. Tsaplev, Anal. Chem. 67 (2012) 506–514.
[6] Y. Mao, Y. Bao, W. Wang, Z. Li, F. Li, L. Niu, Talanta 85 (2011) 2106–2112.
[7] P. Vasileva, B. Donkova, I. Karadjova, C. Dushkin, Colloids Surf. A: Physicochem. Eng. Asp. 382 (2011) 203–210.
[8] Y. Gao, G. Wang, H. Huang, J. Hu, S.M. Shah, X. Su, Talanta 85 (2011) 1075–1080.
[9] C. Hu, S. Hu, J. Sens. 2009 (2009) 1–40.
[10] J. Qu, Y. Shen, X. Qu, S. Dong, Chem. Commun. (2004) 34–35.
[11] X. Zhao, R. Liu, Environ. Int. 40 (2012) 244–255.
[12] M.G. Zhang, A. Smith, W. Gorski, Anal. Chem. 76 (2004) 5045–5050.
[13] F. Patolsky, Y. Weizmann, I. Willner, Angew. Chem. Int. Ed. 43 (2004) 2113–2117.
[14] M. Wang, F. Zhao, Y. Liu, S. Dong, Biosens. Bioelectron. 21 (2005) 159–166.
[15] S. Liu, C. Cai, J. Electroanal. Chem. 602 (2007) 103–114.
[16] J. Wan, J. Bi, P. Du, S. Zhang, Anal. Biochem. 386 (2009) 256–261.
[17] S. Deng, G. Jian, J. Lei, Z. Hu, H. Ju, Biosens. Bioelectron. 25 (2009) 373–377.
[18] J.M. You, Y.N. Jeong, M.S. Ahmed, S.K. Kim, H.C. Choi, S. Jeon, Biosens. Bioelectron. 26 (2011) 2287–2291.
[19] B. Zhang, D. Huang, X. Xu, G. Alemu, Y. Zhang, F. Zhan, Y. Shen, M. Wang, Electrochim. Acta 91 (2013) 261–266.
[20] K. Wusiman, H. Jeong, K. Tulugan, H. Afrianto, H. Chung, Int. Commun. Heat Mass Trans. 41 (2013) 28–33.
[21] R.M. Santos, M.S. Rodrigues, J. Laranjinha, R.M. Barbosa, Biosens. Bioelectron. 44 (2013) 152–159.
[22] M. Iguchi, S. Yamanaka, A. Budhiono, J. Mater. Sci. 35 (2) (2000) 261–270.
[23] (a) F.K. Andrade, N. Alexandre, I. Amorim, F. Gartner, A.C. Mauricio, A.L. Luis, M. Gama, J. Bioact, Compat. Polym. 28 (2012) 97–112;
(b) M.J. Berrocal, I.H.A. Badr, D.Y. Gao, L.G. Bachas, Anal. Chem. 73 (2001) 5328–5333;
(c) C.E. Tom, M.E. Meyerhoff, Anal. Chem. 67 (1995) 3108–3114.
[24] D. Klemm, F. Kramer, S. Moritz, T. Lindstrom, M. Ankerfors, D. Gray, A. Dorris, Angew. Chem. Int. Ed. Engl. 50 (2011) 5438–5466.
[25] S.H. Yoon, H.J. Jin, M.C. Kook, Y.R. Pyun, Biomacromolecules 7 (2006) 1280.
[26] T. Zhou, Express Polym. Lett. 7 (2013) 756–766.
[27] W. Wang, T.J. Zhang, D.W. Zhang, H.Y. Li, Y.R. Ma, L.M. Qi, Y.L. Zhou, X.X. Zhang, Talanta 84 (2011) 71–77.
[28] Y.H. Kim, S. Park, K. Won, H.J. Kim, S.H. Lee, J. Chem. Technol. Biotechnol. 88 (2013) 1067–1070.
[29] J. Yu, T. Zhao, F. Zhao, B. Zeng, Electrochim. Acta 53 (2008) 5760–5765.
[30] C.J. Mao, X.B. Chen, H.L. Niu, J.M. Song, S.Y. Zhang, R.J. Cui, Biosens. Bioelectron. 31 (2012) 544–547.
[31] M. Wang, Y. Shen, Y. Liu, T. Wang, F. Zhao, B. Liu, S. Dong, J. Electroanal. Chem. 578 (2005) 121–127.
[32] Y. Liu, M. Wang, F. Zhao, Z. Guo, H. Chen, S. Dong, J. Electroanal. Chem. 581 (2005) 1–10.
[33] Z. Shi, S. Zang, F. Jiang, L. Huang, D. Lu, Y. Ma, G. Yang, RSC Adv. 2 (2012) 1040.
[34] C. Renault, C.P. Andrieux, R.T. Tucker, M.J. Brett, V. Balland, B. Limoges, J. Am. Chem. Soc. 134 (2012) 6834–6845.
[35] J. Liu, L. Han, T. Wang, W. Hong, Y. Liu, E. Wang, Chem. Asian J. 7 (2012) 2824–2829.
[36] A.J. Bard, L.R. Faulkner, Electrochemical Methods, 2nd ed., John Wiley & Sons, New York, 2001.
[37] E. Laviron, J. Electroanal. Chem. 101 (1979) 19–22.
[38] L. Cui, M. Xu, J. Zhu, S. Ai, Synth. Met. 161 (2011) 1686–1690.
[39] C. Yu, X. Zhou, H. Gu, Electrochim. Acta 55 (2010) 8738–8743.
[40] J. Liu, Y. Li, X. Huang, Z. Zhu, Nanoscale Res. Lett. 5 (2010) 1177–1181.
[41] L. Li, J. Huang, T. Wang, H. Zhang, Y. Liu, J. Li, Biosens. Bioelectron. 25 (2010) 2436–2441.
[42] R. Kamin, G. Wilson, Anal. Chem. 52 (1980) 1198–1205.
[43] Y. Zhou, S. Liu, H. Jiang, H. Yang, H. Chen, Electroanalysis 22 (2010) 1323–1328.